



Accepted Article

Title: Ionic Covalent Organic Frameworks Consisting of Tetraborate Nodes and Flexible Linkers

Authors: Lacey J. Wayment, Shaofeng Huang, Hongxuan Chen, Zepeng Lei, Ashley Ley, Se-Hee Lee, and Wei Zhang

This manuscript has been accepted after peer review and appears as an Accepted Article online prior to editing, proofing, and formal publication of the final Version of Record (VoR). The VoR will be published online in Early View as soon as possible and may be different to this Accepted Article as a result of editing. Readers should obtain the VoR from the journal website shown below when it is published to ensure accuracy of information. The authors are responsible for the content of this Accepted Article.

To be cited as: Angew. Chem. Int. Ed. 2024, e202410816

Link to VoR: https://doi.org/10.1002/anie.202410816



WILEY. VCH

COMMUNICATION

Ionic Covalent Organic Frameworks Consisting of Tetraborate Nodes and Flexible Linkers

Lacey J. Wayment^[a], Shaofeng Huang^[a], Hongxuan Chen^[a], Zepeng Lei^[a], Ashley Ley^[a], Se-Hee Lee^[b], Wei Zhang^[a]*

[a] L. J. Wayment, S. Huang, H. Chen, Dr. Z. Lei, A. Ley, Prof. W. Zhang

Department of Chemistry
University of Colorado Boulder

University of Colorado Boulder

Boulder, CO 80309 (USA)

*E-mail: wei.zhang@colorado.edu

[b] Prof. S.-H. Lee

Department of Mechanical Engineering

University of Colorado Boulder

Boulder, CO 80309 (USA)

Supporting information for this article is given via a link at the end of the document.

Abstract: Covalent organic frameworks (COFs) have emerged as versatile materials with many applications, such as carbon capture, molecular separation, catalysis, and energy storage. Traditionally, flexible building blocks have been avoided due to their potential to disrupt ordered structures. Recent studies have demonstrated intriguing properties and enhanced structural diversity achievable with flexible components by judicious selection of building blocks. This study presents a novel series of ionic COFs (ICOFs) consisting of tetraborate nodes and flexible linkers. These ICOFs use borohydrides to irreversibly deprotonate the alcohol monomers to achieve a high polymerization degree. Structural analysis confirms the dia topologies. Reticulation is explored using various monomers and metal counterions. Also, these frameworks exhibit excellent stability in alcohols and coordinating solvents. The materials are tested as single-ion conductive solid-state electrolytes. ICOF-203-Li displays one of the lowest activation energies reported for ion conduction. This tetraborate chemistry is anticipated to facilitate further structural diversity and functionality in crystalline polymers.

Covalent organic frameworks (COFs) have emerged as an appealing platform for designing innovative materials with diverse applications such as carbon capture, molecular separation, heterogeneous catalysis, and energy storage. [1-6] The customizable structure of these crystalline polymers allows for tailoring them to specific applications by carefully selecting the monomers and linkages. Typically, COFs are designed using dynamic covalent chemistry (DCvC) and the principle of reticulation. The principle of reticulation dictates that molecular building blocks maintain a known geometry within the crystal lattice, while DCvC enables error correction during the polymerization to favor ordered networks. [7,8] With these principles, there has been tremendous success in designing highly crystalline polymetric architectures using rigid linkages and monomers. [9]

On the other hand, flexible monomers or linkages have traditionally been avoided in the design of crystalline materials due to their tendency to disrupt the thermodynamic drive toward ordered structures by introducing additional degrees of rotation. [10-13] Recent studies have shown that employing flexible monomers or linkages can lead to intriguing properties and enhance structural diversity. For instance, Fang et al. observed topological isomerization by using 4,4',4",4"'-([9,9'-bicarbazole]-3,3',6,6'-tetrayl)tetrabenzaldehyde (BCTB-4CHO) as a monomer, which exhibits a low energy barrier for adopting a wide range of dihedral angles.[14] This flexibility allowed them to create dia net and qzt net structures with distinct properties. Another example is the spiroborate linkage, which has been used to form 1D and 3D polymers where the dihedral angle of the boron center can be varied from 66° to 90° due to the flexibility of the B-O bonds.[15-19] In all cases, the design requires a judicious selection of building blocks to achieve desired topologies.

Here, we present the synthesis and characterization of a novel series of ionic COFs (ICOFs) consisting of tetraborate nodes and flexible linkers. The design of these materials demonstrates how flexibility can be introduced into the node and linker while maintaining a predictable topology. Structural analysis confirms that the new series adopts *dia* topologies. The reticulation of this unique chemistry is explored with three different monomers and by varying the metal counter-ion. These frameworks exhibit excellent chemical stability in alcohols and coordinating solvents.

Moreover, an emerging strategy for improving the performance of solid polymer electrolytes involves generating ion hopping sites within ordered channels, similar to solid inorganic electrolytes. [20,21] These sites serve to uncouple cation conduction from the motion within the polymer chains, thereby enhancing conductivity. There has been much success in developing ICOF solid state electrolytes using this approach. [22-26] Furthermore,

Jibrary for rules of use; OA articles are governed by the applicable Creative Commons License

COMMUNICATION

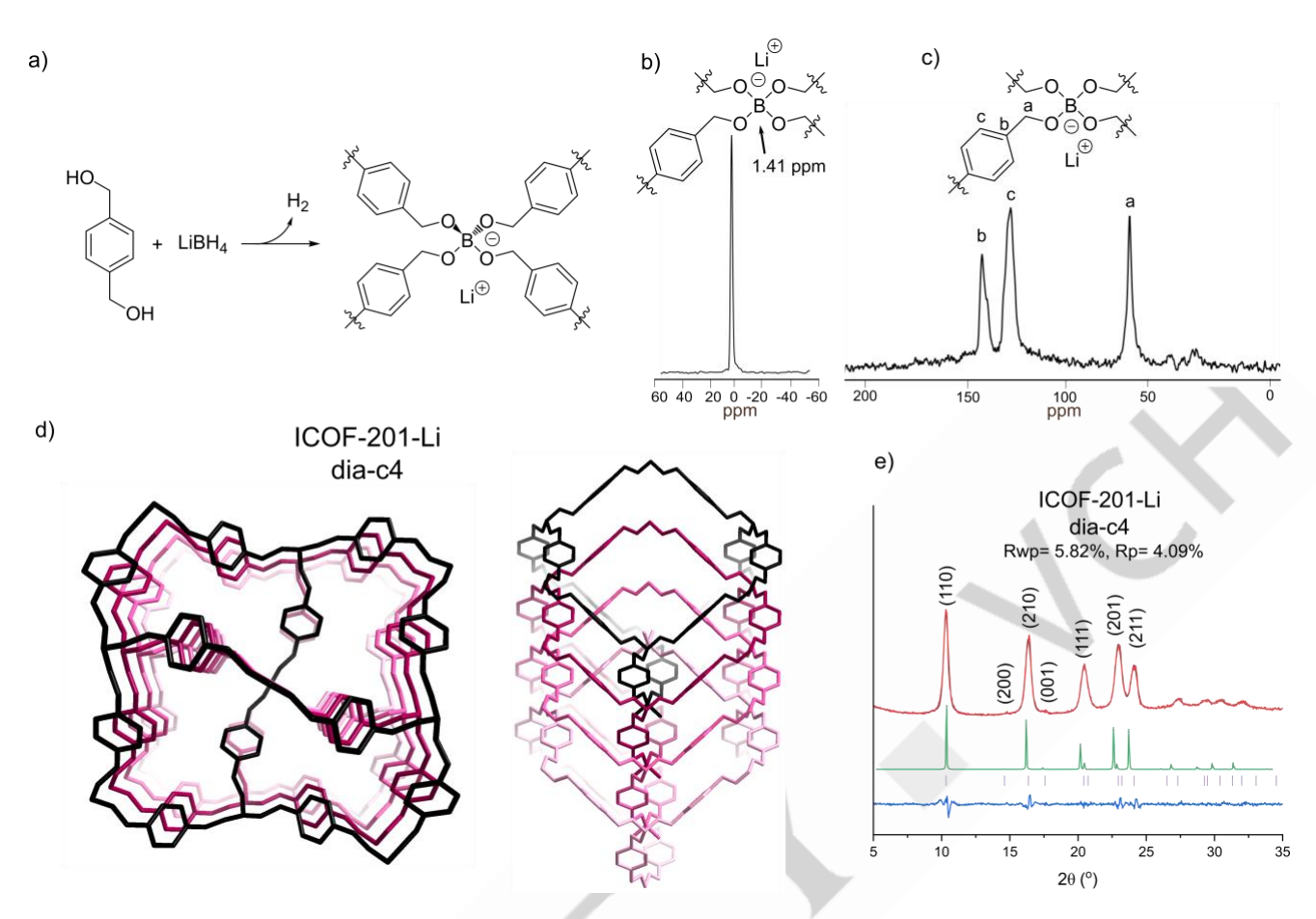


Figure 1. Synthesis and characterization of ICOF-201-Li. (a) The synthetic scheme of ICOF-201-Li which forms tetrahedral nodes at the boron center. Solid-state ¹¹B (b) and ¹³C (c) NMR of ICOF-201-Li. (d) ICOF-201-Li forms a four-fold interpenetrated *dia* topology. (e) Pawley refinement (black) of ICOF-201-Li. The experimental pattern (red) with the difference (light blue) and the Bragg reflections (purple). The simulation of the *dia* topology model with four-fold interpenetration is shown in green.

there is growing research interest in sodium ion batteries. The abundance of sodium, lower cost, and similar energy storage mechanism make it an attractive alternative to lithium ion batteries. [27-30] The tetraborate platform in this work has great potential in advancing this research effort due to the ease of tunability of both the linkers and metal ions. These ICOFs exhibit one of the lowest activation energies for ion conduction. We anticipate that this methodology can be broadly applied to other monomers. Many aldehyde monomers have been developed that could be easily transformed into alcohols. Thus, this chemistry will further the structural diversity of crystalline polymers and lead to the discovery of novel properties.

The conventional formation of charged borate species involves using boron sources like trimethyl borate or boric acid, along with a base. For spiroborate formation, the monomer design necessitates a catechol or diol monomer capable of chelating the boron center. The conversion rate was notably low when this approach was employed to synthesize ICOF-201-Li from 1,4-benzenedimethanol. This is likely due to the absence of a chelating interaction as a thermodynamic driving force to favor polymerization. So, in a closed system, there is limited driving force toward the polymerization. To overcome such limitation, the

traditional boron reagents were replaced with lithium borohydride (LiBH₄). Irreversibly deprotonating the alcohol monomers dramatically enhanced the kinetic driving force toward polymerization, while dynamic B-O bond exchange can still enable the error correction behavior.

ICOF-201-Li synthesis involved the reaction of LiBH4 with 1,4-benzenedimethanol in benzonitrile at 150 °C for 7 days (Figure 1a). Fourier-transform infrared spectroscopy (FT-IR) evidenced the formation of a B-O bond at 1066 cm⁻¹, along with the complete reduction of the -OH stretch at 3268 cm⁻¹ (Figure S1). Solid-state ¹¹B NMR revealed a single boron species at 1.41 ppm, which is similar to other alcohol based small molecules^[20,21] (Figure 1b). Solid-state ¹³C NMR displayed three carbon species, consistent with the expected structure (Figure 1c). SEM showed the morphology of the polycrystalline sample to be clusters of rods (Figure S2). We expected the topology of ICOF-201-Li to be a dia net. To determine if this was the appropriate topology, dia models were created ranging from being non-interpenetrated to six-fold interpenetrated (Figure S3).[7] The experimental pattern matches well with the four-fold interpenetrated structure (Figure 1d and 1e). The cell dimensions were found to be a=b= 12.1098 Å and c=

WILEY. VCH

COMMUNICATION

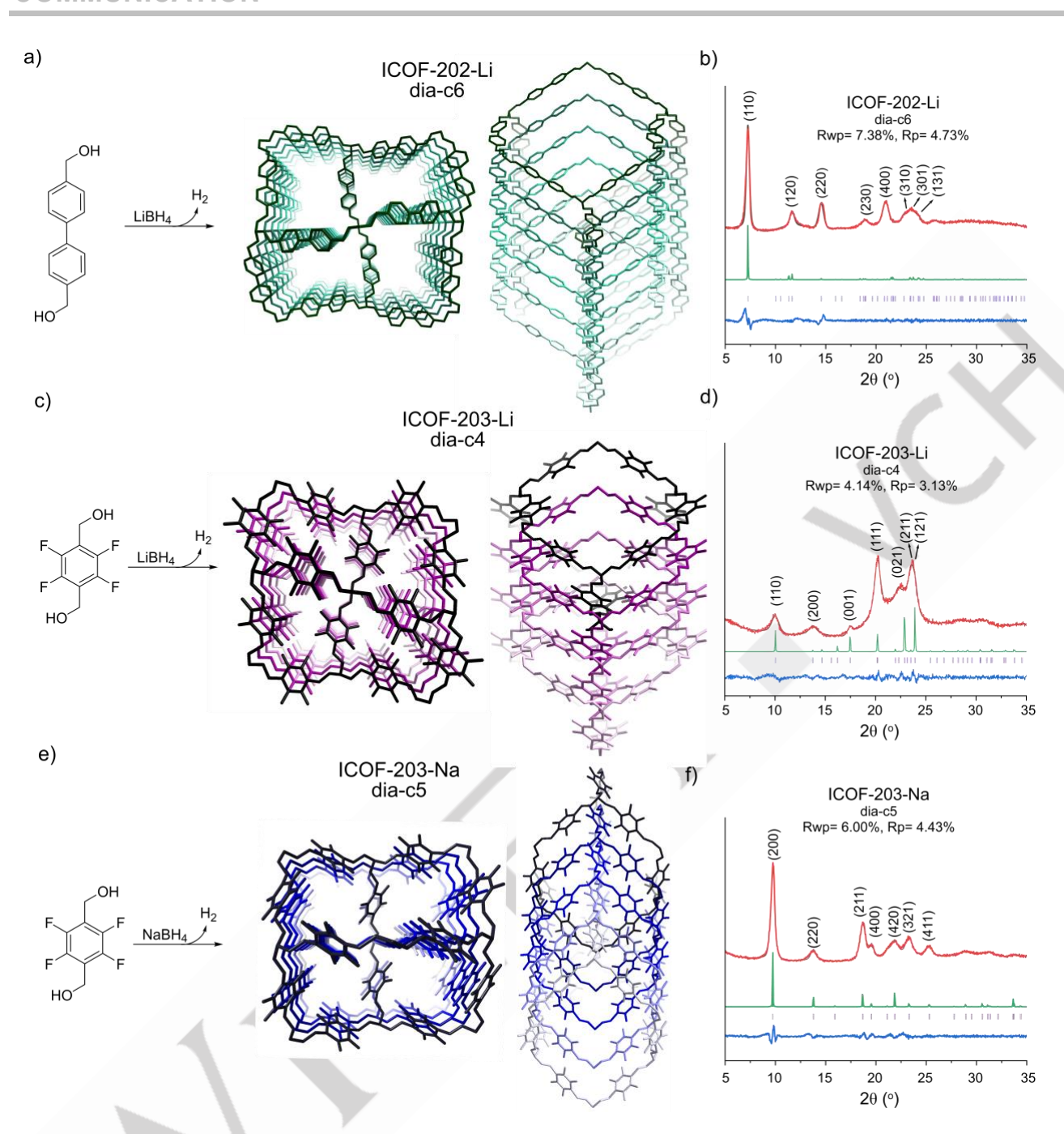


Figure 2. Synthesis and topology of ICOF-202-Li, ICOF-203-Li, and ICOF-203-Na. Synthetic scheme of ICOF-202-Li (a), ICOF-203-Li (c), and ICOF-203-Na (e). Pawley refinement (black) of ICOF-202-Li (b), ICOF-203-Li (d), and ICOF-203-Na (f) overlayed with the experimental patterns (red). The difference (light blue), the Bragg reflections (purple), and the simulation of the respective dia topology model (green) are also included.

5.03920 Å in a tetragonal crystal lattice with a space group of $P\bar{4}b2$ after Pawley Refinement (R_{wp}= 5.82% and R_p= 4.09%).

Next, the reticulation and scope of this tetraborate chemistry were explored by varying the molecular building blocks. 3D frameworks are often considered challenging due to the difficulty in controlling interpenetration and topology. [6] It has been reported that longer linkers generally result in higher-level interpenetration. [33,34] Still, non-covalent interactions and the size of counter-ions can change the level of interpenetration. [35-40] Additionally, alkali metals have been shown to play a critical role

in the observed topology in ionic crystalline polymers by introducing metal-coordination bonds. [19,41] Thus, ICOF-202-Li (Figure 2a) and ICOF-203-Li (Figure 2c) were synthesized using 4,4'- bis(hydroxymethyl)biphenyl and 2,3,5,6,-tertrafluoro-1,4-benzenedimethanol to explore the effect of length on the topology. While sodium borohydride (NaBH₄) replaced LiBH₄ to test the effect of counter-ion when creating ICOF-203-Na (Figure 2e). The chemical characterization and morphology analysis yielded results akin to those observed for ICOF-201-Li (SI Section 4).

WILEY VCH

COMMUNICATION

ICOF-202-Li's experimental diffraction pattern was compared to varying levels of interpenetration in the \emph{dia} topology and matched the six-fold interpenetration well (Figure S7). The space group assigned to this model was Pnn2. The dimensions of the unit cell were determined to be a = 16.8265 Å, b = 17.6382 Å, and c = 4.87010 Å (Pawley refinement, R_{wp} = 7.38% and R_p = 4.73%) (Figure 2b). This suggests that increasing the length of the linker will increase the interpenetration. Others have observed that greater distances between tetrahedral centers can result in higher levels of interpenetration. $^{[34]}$

Next, ICOF-203-Li was chosen to evaluate the compatibility of this tetraborate chemistry with other functional groups while keeping the monomer length the same. The fluorine on the monomer will reduce the Lewis basicity of the alcohols, but the framework is still formed with good yield. The experimental diffraction pattern was compared to various dia nets and aligned most closely with a four-fold interpenetrated with a space group of Pba2 (Figure S11). Following Pawley refinement, the unit cell dimensions were determined as a = 12.8783 Å, b = 12.0796 Å, and c = 5.0743 Å (Figure 2d). Notably, the orientation of the

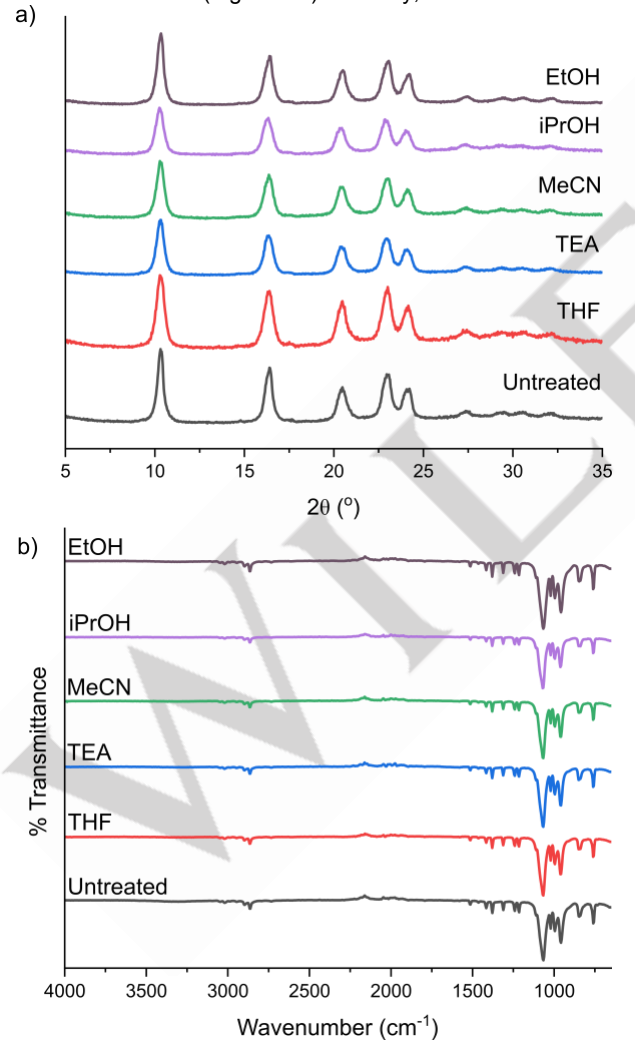


Figure 3. Comparison of ICOF-201-Li PXRD (a) and FT-IR (b) after various chemical treatments

linkers impacted the intensity of the peaks, as evidenced in the comparison between ICOF-203-Li and ICOF-203-Na (Figure 2d and 2f). The simulations revealed a closer match to the experimental pattern of ICOF-203-Li when the orientation of the aromatic ring is relatively flat. Conversely, in ICOF-203-Na, signal intensity was better matched when the aromatic ring was angled (Figure 2e). Additionally, ICOF-203-Na exhibited a five-fold interpenetrated structure (Figure S15). Following Pawley refinement, the dimensions of the unit cell were found to be a = b = 18.1731 Å and c = 5.854 Å, with $R_{\rm wp}$ at 6.00% and $R_{\rm p}$ at 4.43% (Figure 2f). This change in interpenetration could be due to the sodium ions increasing the spacing between the tetraborate centers in the c-axis of the unit cell. This causes the relative length of the flexible linker to be increased, thus favoring a higher interpenetrated structure.

Next, the stability and porosity of the 3D tetraborate frameworks were tested. ICOF-201-Li was tested against a variety of solvents, such as alcohols and coordinating solvents, by soaking the ICOF in the solvents for 16 hours. After that period, the solvent was removed, and the resulting solid was subjected to characterization. PXRD showed that crystallinity is retained after all solvent treatments (Figure 3a), and FT-IR showed no evidence of degradation (Figure 3b). The other ICOFs also remained largely unaffected by the same chemical treatment (SI Section 5). When the ICOFs were soaked in water, only ICOF-201-Li retained most of its crystallinity. The PXRD and FT-IR showed evidence of minimal hydrolysis (Figure S19). Next, thermogravimetric analysis (TGA) was used to evaluate thermal stability. ICOF-201-Li showed a minor mass loss of less than 10 wt% until 435 °C (Figure S23). The stability of the other ICOFs was slightly lower because the mass loss of 10 wt% ranged from 300 to 420 °C (Figure S23). The porosity of the ICOFs was tested by measuring the nitrogen isotherm (SI Section 6). ICOF-201-Li and ICOF-203-Li are predicted to have inaccessible micropores (Figure S20 and Figure S22). However, they still have measurable BET surface areas of 107 m² g⁻¹ and 219 m² g⁻¹, respectively. Analysis of the pore size distribution shows mesopores that likely stem from the morphology, which consists of clusters of needle-like crystals (Figure S2 and Figure S10). This demonstrates that synthetic conditions can play an important role in observed properties. On the other hand, ICOF-202-Li and ICOF-203-Na have measurable micropores that match well with the proposed topologies and show slightly higher surface areas of 155 m² g⁻¹ and 231 m² g⁻¹, respectively (Figure S21 and S23). We attribute the presence of the micropores in ICOF-203-Na, but not in ICOF-203-Li, to the change in topology and orientation of the flexible linker due to the difference in counter ion. These results demonstrate that fairly robust and porous frameworks can be constructed from simple building blocks via tetraborate chemistry.

Finally, we evaluated the ICOFs as solid-state electrolytes (SSE). The structure-activity relationship of the initial series of ICOF-200s was evaluated to understand how the structural features affect the ion conductivity. Prior to all measurements, the ICOFs were dried in a vacuum oven overnight at 120 °C. Then, a

WILEY. vch

COMMUNICATION

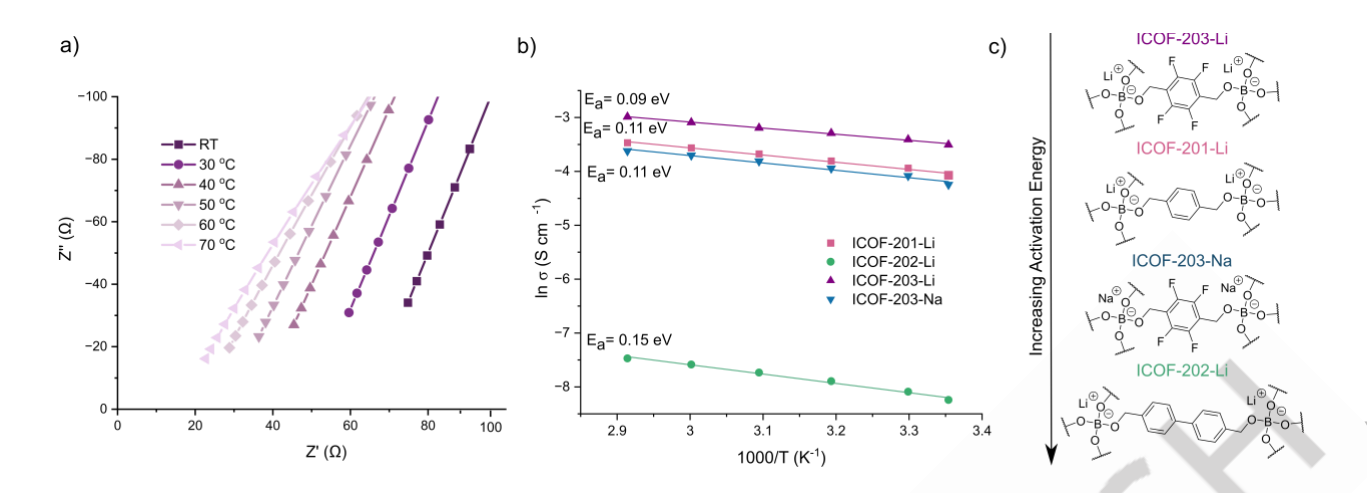


Figure 4. Structure-activity relationship of ICOF-201-Li to ICOF-203-Na (a) Nyquist plot of ICOF-203-Li at different temperatures. (b) Arrhenius plot of ICOF-201-Li to ICOF-203-Na with the calculated activation energy in eV per atom. (c) Repeating units of the ICOF-201-Li to ICOF-203-Na in order of activation energy.

pellet of the respective ICOFs was created with 20 wt% of PYR13FSI, an environmentally friendly plasticizer.^[42]

Electrochemical impedance spectroscopy was used to measure the ion conductivity across a temperature gradient (Figure 4a and Figure S24). Arrhenius plots were created to calculate the activation energy for ion transport in each ICOF to understand the relationship between the structures and ion transportation (Figure 4b). ICOF-203-Li was found to have the lowest energy barriers of 0.09 eV per atom (Figure 4c). ICOF-201-Li has the next lowest activation energy for lithium ion transport, suggesting the fluorine on the backbone can facilitate ion transport through the material. The fluorine could contribute to the ion conductivity in two ways. First, the electronegativity of fluorine can weaken the electrostatic attraction between the tetraborate group and counter ion, thus making the ions more mobile. Additionally, fluorine can act as a hopping site to facilitate ion conduction (Figure 4c). Increasing the length of the flexible linker appears to be detrimental when comparing the activation energy for ion transport in the ICOF-201-Li and ICOF-202-Li frameworks (Figure 4b). When the counter ion is changed from lithium to sodium the activation energy of ion conduction increases to 0.11 eV. This is due to sodium ions having a greater mass.

Further exploration of ICOF-203-Li showed that the lithium transference was 0.93 when using the Bruce-Vincent-Evans technique (Figure S26). A high transference will improve the energy efficiency of the battery by reducing the buildup of ion gradients and lithium dendrite growth. [43-45] Additionally, linear sweep voltammetry shows ICOF-203-Li is stable up to ~4.5V, which suggests that it is compatible with high-voltage cathode material (Figure S26). Table 1 summarizes the ion conductivity at 30 °C and activation energy of the four ICOFs. It is anticipated that monomer designs can be tuned to improve the properties further.

Table 1. Summary of ion conductivity data of ICOF electrolytes at 30 °C and the respective activation energies.

ICOF	σ (S cm ¹) at 30 °C	E _a (eV/atom)
ICOF-201-Li	1.2 x10 ⁻⁴	0.11
ICOF-202-Li	3.1 x10 ⁻⁴	0.15
ICOF-203-Li	3.9 x10 ⁻⁴	0.09
ICOF-203-Na	8.3 x10 ⁻⁵	0.11

In conclusion, this work has demonstrated a novel boron chemistry that creates ICOFs consisting of tetraborate nodes with flexible monomers. The synthesis requires borohydrides to irreversibly deprotonate the alcohol monomers to achieve a high polymerization degree, while the dynamic B-O bonds enable error correction to ensure the formation of crystalline polymers with long-range order. Variation in the monomers and metal ions utilized reveals how the interpenetration and monomer orientation will affect the experimental diffraction pattern. Notably, these frameworks exhibit good chemical and thermal stability. Finally, the impedance of the reported structure was tested to demonstrate the potential of this platform for developing solidstate electrolytes. ICOF-203-Li showed one of the lowest activation energies reported in literature. Incorporating the tetraborate moieties opens avenues for further exploration and diversification of crystalline polymers, indicating a promising direction for future research.

Supporting Information

The data that support the findings of this study are available in the supplementary material of this article.

WILEY VCH

COMMUNICATION

Acknowledgements

W. Z. thanks the support from National Science Foundation (CHE-2108197).

Keywords: Dynamic Covalent Chemistry • Tetraborate• Ionic Covalent Organic Frameworks• Flexible Linkers• Dynamic B-O bonds

References

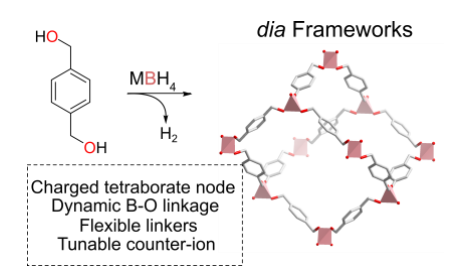
- [1] K. Geng, T. He, R. Liu, S. Dalapati, K. T. Tan, Z. Li, S. Tao, Y. Gong, Q. Jiang, D. Jiang, Chem. Rev. 2020, 120, 8814-8933.
- [2] X. Feng, X. Ding, D. Jiang, *Chem. Soc. Rev.* **2012**, *41*, 6010-6022.
- [3] S.-Y. Ding, W. Wang, *Chem. Soc. Rev.* **2013**, *42*, 548-568.
- [4] C. S. Diercks, O. M. Yaghi, Science 2017, 355, eaal1585.
- [5] Y. Jin, Y. Hu, W. Zhang, Nat. Rev. Chem. 2017, 1, 0056.
- [6] X. Guan, F. Chen, Q. Fang, S. Qiu, Chem. Soc. Rev. 2020, 49, 1357-1384.
- [7] M. O'Keeffe, M. A. Peskov, S. J. Ramsden, O. M. Yaghi, Acc. Chem. Res. 2008, 41, 1782-1789.
- [8] Y. Jin, C. Yu, R. J. Denman, W. Zhang, Chem. Soc. Rev. 2013, 42, 6634-6654.
- [9] L. J. Wayment, Z. Lei, Y. Jin, W. Zhang, CCS Chem. 2023, 5, 2194-2206.
- [10] L. Xu, S.-Y. Ding, J. Liu, J. Sun, W. Wang, Q.-Y. Zheng, Chem. Commun. 2016, 52, 4706-4709.
- [11] C. Zhao, C. S. Diercks, C. Zhu, N. Hanikel, X. Pei, O. M. Yaghi, J. Am. Chem. Soc. 2018, 140, 16438-16441.
- [12] X. Han, Q. Xia, J. Huang, Y. Liu, C. Tan, Y. Cui, J. Am. Chem. Soc. 2017, 139, 8693-8697.
- [13] Z. Lei, L. J. Wayment, J. R. Cahn, H. Chen, S. Huang, X. Wang, Y. Jin, S. Sharma, W. Zhang, J. Am. Chem. Soc. 2022, 144, 17737-17742.
- [14] Y. Liu, J. Li, J. Lv, Z. Wang, J. Suo, J. Ren, J. Liu, D. Liu, Y. Wang, V. Valtchev, S. Qiu, D. Zhang, Q. Fang, J. Am. Chem. Soc. 2023, 145, 9679-9685.
- [15] Y. Du, H. Yang, J. M. Whiteley, S. Wan, Y. Jin, S.-H. Lee, W. Zhang, Angew. Chem. Int. Ed. 2016, 55, 1737-1741.
- [16] Y. Hu, S. J. Teat, W. Gong, Z. Zhou, Y. Jin, H. Chen, J. Wu, Y. Cui, T. Jiang, X. Cheng, W. Zhang, Nat. Chem. 2021, 13, 660-665.
- [17] X. Wang, M. Bahri, Z. Fu, M. A. Little, L. Liu, H. Niu, N. D. Browning, S. Y. Chong, L. Chen, J. W. Ward, A. I. Cooper, J. Am. Chem. Soc. 2021, 143, 15011-15016.
- [18] L. J. Wayment, X. Wang, S. Huang, M. S. McCoy, H. Chen, Y. Hu, Y. Jin, S. Sharma, W. Zhang, J. Am. Chem. Soc. 2023, 145, 15547-15552.
- [19] L. J. Wayment, S. J. Teat, S. Huang, H. Chen, W. Zhang, *Angew. Chem. Int. Ed.*, **2024**, *63*, e202403599.
- [20] V. Bocharova, A. P. Sokolov, Macromolecules, 2020, 53, 4141-4157.
- [21] M. A. Stolberg, B. A. Paren, P. A. Leon, C. M. Brown, G. Winter, K. Gordiz, A. Concellón, R. Gómez-Bombarelli, Y. Shao-Horn, J. A. Johnson, J. Am. Chem. Soc. 2023, 145, 16200-16209.
- [22] Y. Hu, L. J. Wayment, C. Haslam, X. Yang, S.-H. Lee, Y. Jin, W. Zhang, EnergyChem, 2021, 3, 100048.
- [23] Y. Zhu, Q. Bai, S. Ouyang, Y. Jin, W. Zhang, ChemSusChem 2024, 17, e202301118.
- [24] D. Zhu, G. Xu, M. Barnes, Y. Li, C.-P. Tseng, Z. Zhang, J.-J. Zhang, Y. Zhu, S. Khalil, M. M. Rahman, R. Verduzco, P. M. Ajayan, *Adv. Funct. Mater.* 2021, 31, 2100505.
- [25] X. Zhao, P. Pachfule, A. Thomas, *Chem. Soc. Rev.* **2021**, *50*, 6871-6913.
- [26] X. Liang, Y. Tian, Y. Yuan, Y. Kim, *Adv. Mater.* **2021**, *33*, 2105647.
- [27] P. Albertus, S. Babinec, S. Litzelman, A. Newman, Nat. Energy 2018, 3, 16-21.
- [28] S. F. Schneider, C. Bauer, P. Novák, E. J. Berg, Sustain. Energy Fuels 2019, 3, 3061-3070.
- [29] K. Abraham, ACS Energy Lett. 2020, 5, 3544-3547.
- [30] W. Zhang, J. Lu, Z. Guo, *Mater. Today* **2021**, *50*, 400-417.
- [31] M. Moriya, D. Kato, W. Sakamoto, T. Yogo, Chem. Commun. 2011, 47, 6311-6313.

- [32] D. T. Duncan, B. Roy, S. L. Piper, C. Nguyen, P. Howlett, M. Forsyth, D. R. MacFarlane, J. Sun, M. Kar, J. Phys. Chem. C 2022, 126, 18918-18030
- [33] F. J. Uribe-Romo, J. R. Hunt, H. Furukawa, C. Klöck, M. O'Keeffe, O. M. Yaghi, J. Am. Chem. Soc. 2009, 131, 4570-4571.
- [34] T. Ma, J. Li, J. Niu, L. Zhang, A. S. Etman, C. Lin, D. Shi, P. Chen, L.-H. Li, X. Du, J. Sun, W. Wang, J. Am. Chem. Soc. 2018, 140, 6763-6766.
- [35] Y. Liu, Y. Ma, Y. Zhao, X. Sun, F. Gándara, H. Furukawa, Z. Liu, H. Zhu, C. Zhu, K. Suenaga, P. Oleynikov, A. S. Alshammari, X. Zhang, O. Terasaki, O. M. Yaghi, *Science* 2016, 351, 365-369.
- [36] Y. Liu, Y. Ma, J. Yang, C. S. Diercks, N. Tamura, F. Jin, O. M. Yaghi, J. Am. Chem. Soc. 2018, 140, 16015-16019.
- [37] Y. Xie, J. Li, C. Lin, B. Gui, C. Ji, D. Yuan, J. Sun, C. Wang, J. Am. Chem. Soc. 2021, 143, 7279-7284.
- [38] X. Wu, X. Han, Y. Liu, Y. Liu, Y. Cui, J. Am. Chem. Soc. 2018, 140, 16124-16133.
- [39] Y. Wang, Y. Liu, H. Li, X. Guan, M. Xue, Y. Yan, V. Valtchev, S. Qiu, Q. Fang, J. Am. Chem. Soc. 2020, 142, 3736-3741.
- [40] Y. Xiao, Y. Ling, K. Wang, S. Ren, Y. Ma, L. Li, J. Am. Chem. Soc. 2023, 145, 13537-13541.
- [41] S. Fischer, J. Roeser, T. C. Lin, R. H. DeBlock, J. Lau, B. S. Dunn, F. Hoffmann, M. Fröba, A. Thomas, S. H. Tolbert, *Angew. Chem. Int. Ed.* 2018, 57, 16683-16687.
- [42] Y. Hu, N. Dunlap, H. Long, H. Chen, L. J. Wayment, M. Ortiz, Y. Jin, A. Nijamudheen, J. L. Mendoza-Cortes, S.-H. Lee, W. Zhang, CCS Chem. 2021, 3, 2762-2770.
- [43] B. M. Wiers, M.-L. Foo, N. P. Balsara, J. R. Long, J. Am. Chem. Soc. 2011, 133, 14522-14525.
- [44] J. F. Van Humbeck, M. L. Aubrey, A. Alsbaiee, R. Ameloot, G. W. Coates, W. R. Dichtel, J. R. Long, *Chem. Sci.* 2015, 6, 5499-5505.
- [45] H. Zhang, C. Li, M. Piszcz, E. Coya, T. Rojo, L. M. Rodriguez-Martinez, M. Armand, Z. Zhou, Chem. Soc. Rev. 2017, 46, 797-815.

WILEY VCH

COMMUNICATION

Entry for the Table of Contents



A tetraborate node has been shown to facilitate the formation of 3D ionic covalent organic frameworks with flexible linkers. Irreversible deprotonation acts as a kinetic control to achieve high polymerization, while the dynamic B-O bond aids error correction. This approach has been investigated with three organic monomers and two metal counterions.

Institute and/or researcher Twitter usernames:

Wei Zhang: @weizhangCU

CU Boulder Chemistry: @CUBoulderCHEM